Non-contact Inspection of Worm and Worm wheel using a Vision system

M. B. Kiran
Associate Professor,
Department of Mechanical Engineering,
School of Technology, Pandit Deendayal Energy University,
MB.Kiran@sot.pdpu.ac.in

Abstract

Worm gears are used in industries where fast stopping and breaking applications such as lifts, hoists, and elevators. Worm gears are also used in machine tools. Worm gear sets are typically used in the gearbox. Worm gear motors offer quietness when compared to other types of equipment. They require small gearboxes, and they are increasingly used in space-saving applications. Inspection of worm gears is significant before they are deployed into service. This would ensure that they will not fail when put into service. Many of the existing gear inspection techniques are post-process in nature, and hence they are not fit for 100% inspection of gears. The current research work attempts to design and develop a novel approach for the non-contact assessment of worm gears using a vision system. Validation of the results obtained by the current method is done by comparing them with the results of the standard technique. As far as the author's knowledge goes, no research article reported on the worm gear inspection using a vision system. In this context, the present research assumes special significance. The accuracy obtained by the current process is 98%. The method has shown very high repeatability. The way finds application in the online inspection of worm gears. The research investigation revealed that the technique could detect damaged teeth and other defects such as Wear, scoring, pitting, and fracture, with a classification accuracy of 93.33%, 94.66%, 94%, 94.66%, and 100%, respectively.

Keywords
Worm gear, Worm wheel, Worm gear Inspection, Non-contact inspection, Vision inspection

1. Introduction

Worm and Worm wheel is being used in multiple applications such as lifts, hoists, elevators, machine tools, etc. In machine tools, they are used in drives for rotary indexing tables. This application requires high positioning accuracy, and elimination of backlash is critical. They are also used in turbine governor drives. Worm gears are now being made by additive manufacturing. Worm gears are generally used for transmitting motion when the shafts are nonparallel. Worm gears can be used up to 24000 rpm. The main advantage of worm gears is that they operate quietly when put into service. And they have a very high gear reduction ratio and occupy less space. Hence significant speed reductions are possible using worm and worm wheel in a single stage. A worm wheel is usually made using brass, and the worm is made using steel. Worms are generally made harder than worm wheels. This will prevent wear on the worm. The main problem with worm gears is that it is tough to lubricate. This is because the movement between worm and worm wheel is entirely sliding. Also, the lubricants used with the worm wheel require very high viscosity. This makes filtering fats a big challenge. Also, viscosity is the main factor that prevents the worm from touching the worm wheel in a worm gear set. ISO 460 and ISO 680 are the most commonly used lubricants in the worm gear set. In many applications related to worm gear sets, mineral-based compounded gear oils. The lubricants prevent the sliding wear of the worm gear set. Thus, by using lubricants, direct metal-to-metal contact may be prevented. Some applications use additives such as natural or synthetic fatty acids to increase lubrication efficiency. Mineral oil-based extreme pressure oil is also being used in some applications Polyalphaolefin provides excellent lubrication with a worm gear set. Polyalkylene glycols are also being used as a lubricant in worm gear sets. The worm wheel wears out more quickly than the worm in a worm gear set. This is because the worm wheel is made out of softer material. Using a sulfur-phosphorous EP gear oil at high temperatures might activate EP additives. When EP additive starts will cause an oxide layer will form on the steel worm, which will protect the gear tooth from shock loads. On the other hand, the EP additive activation would result in severe corrosion on the worm wheel, as it is made out of brass. This corrosion of the brass worm wheel is because of sulfur. Some applications might use steel worm and steel worm wheels. However, this kind of worm gear set is not vulnerable to corrosion, as, in the case of brass, the gearbox repairs would become costly also time-consuming. Moderate to light load applications typically use brass worm and brass worm wheel. The main advantage of using this combination is that lubrication oil selection is more accessible. When the load is relatively less, plastic on metal /or metal on plastic will be used. The type of lubricant used would depend upon the type of plastic used. Care should be taken while selecting the lubricant so that it will not react with the plastic.

With the advent of additive manufacturing (AM), many worm and worm wheel combination is being made by AM process. AM-made gears have high impact resistance, wear resistance, and self-lubricating properties. Nowadays, many applications use AM-made gears. Usually, a worm will have rack-type teeth, whereas a worm wheel will have involute teeth. Figure 1 shows a typical worm and worm wheel arrangement.

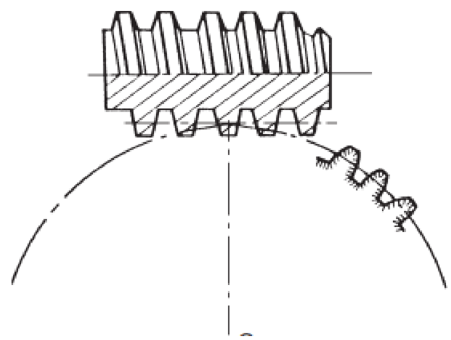

Fig 1 Worm and Worm wheel arrangement

2. Literature review

While manufacturing gears, many simple instruments such as micrometer calipers, height gauges (Thoen 2001), and dial indicators are used to inspect gears (Hoover 2000). This would ensure defect-free gear production. Before the final delivery of gears, they are inspected for defects using Coordinate measuring machines (CMM), and Gear measuring instruments (GMI) are used (Moderow 1992). These are mainly used for the dimensional measurement of worm and worm wheels (Goch 2003). Both GMI and CMM are being used for performing single flank and double flank rolling tests. The test gear will be made to work with a master gear during single and double flank tests. A single flank rolling test expresses results as a sinusoidal graph. The graph would provide information on factors affecting the profile, gear run-out, accumulated pitch, and pitch using Fourier transform. Tooth spacing plays a vital role in terms of contact stress. Research showed that a gear tooth spacing error of 1.5 µm would result in a 50% increase in contact stresses (Simon 2006). Inspection of gears for quality is not only expensive but also time-consuming (Goch 2003). The quality of gears is mainly assessed by the noise and the bearing area of the mating gears. The quality expectations have increased significantly over these years (VDI 2001, AGMA 2002, AGMA 2005).

A double flank rolling test would measure the variation in the distance between the center of the test gear and the center of the master gear during rolling for one complete revolution without backlash (Reiter 2014). The test would generate a sinusoidal graph, which would specify the problems related to the damaged teeth and manufacturing process problems.

To overcome the drawbacks of the tactile methods described above,, optical methods using laser line triangulation came into being (Ni 2019). The triangulation method may also have inaccuracies due to the reflections from gear surfaces (Auerswald 2019). Laser interferometry helps in achieving better scanning speed (Balzer 2015). Gear quality is measured by the noise (acoustic emission) produced during operation (Qu 2014). One of the significant advantages of using the acoustic-based technique for the gear quality assessment is that the method is less sensitive to background noise.

All the techniques mentioned above are post-process and consume s more time. But, the modern-day industries demand 100% inspection of gears. In this context, the present method assumes special significance. The proposed method uses a vision system for the quality inspection of gears.

Many defects such as pitting, wear, scoring, and fracture might happen during gear manufacturing. Hence, there is a need for gear inspection before delivering the gear for actual service. An effort has been made in the current research for identifying the different types of defects in the manufacture of gears.

2.1 Worm elements.

Axial pitch deviation is the difference between the design pitch and the actually measured pitch.
Cyclic error: The error that is observed during each revolution of the worm
Lead deviation: The difference between the design lead and the measured lead or helix
Profile deviation: The difference between the design profile and the measured profile.
Transverse pitch: The measurement taken from one angle to the next at the same radial distance

2.2 The Worm wheel elements

Adjacent pitch deviation: The difference between the design and the actually measured pitch of the consecutive pitches
Cumulative pitch deviation is the difference between the design and measured dimensions of any two teeth more than one pitch apart.
Profile error: in a worm wheel, a tooth flank is imposed by the cutter with which the gear is generated.
The pitch diameter of the worm (D_w) is given by

$$\mathrm{Dw} = \frac{\mathrm{ZwPn}}{\pi\, sin\lambda} \tag{1}$$

Where,
Zw is the number of threads of the worm

The pitch diameter of the worm wheel (D_g) is given by

$$\mathrm{Dw} = \frac{\mathrm{ZgPn}}{\pi\, cos\lambda} \tag{2}$$

Where,
Zg is the number of teeth of the worm wheel/gear

L is the lead of the worm.

$$\mathrm{L} = \frac{\mathrm{ZwPn}}{\pi\, cos\lambda} \tag{3}$$

Where ‘λ’ is the lead angle.

$$\lambda = \mathrm{Arcsin}\frac{\mathrm{ZwPn}}{\pi\, dw} \tag{4}$$

$$\mathrm{Pn} = \mathrm{Px}\ \cos\Upsilon \tag{5}$$

3.Methodology

3.1 Specimen preparation

Worm gears and worm wheels are selected to have different modules. Table 1 shows the specification of the sample worm and worm wheels used in the current research.

Table 1. Technical specification of sample worm and worm wheels.

Number of teeth-Worm wheels	36
Number of teeth-Worm gear	2
Module (mm)	4
Reference circle diameter(mm)	144
Profile shift coefficient(mm)	0
Pressure angle (^{0})	20
Center distance (mm)	90
Helix	Right-hand
Flank type	ZN

3.2Setting up of Vision system

The vision system (Figure 2) consists of a charged coupled device (CCD) used to acquire worm and worm wheels images (1600 x 1236 pixels). The vision system is also fitted to an advanced image processing card. The card would help in efficiently performing the image processing operations. The vision system also will use structured lighting for illuminating the test specimens. A-frame grabber, connected to the vision system, would help digitize the analog signal obtained from the CCD camera.

3.3 Experimentation

The worm wheel (specimen) is kept on the mountable, illuminated using structured lighting, and an image is captured and stored during experimentation. Table 2 shows the digital image of the worm wheel. Similarly, the worm is again kept on the mount table, and the image is captured using a CCD camera. Table 3 shows the digital image of the worm. The experiment is then repeated using different modules/sizes of worm and worm wheels, and an image is grabbed using the CCD camera each time.

3.3.1 Defect identification

Texture features are extracted from the digital image through a co-occurrence matrix ([a]Kiran 2021, [b]Kiran 2021, [c]Kiran 2021, [d]Kiran 2021, Haralick 1973). Texture features obtained from the co-occurrence matrix are used to identify defects and classify worm gears into different classes- G=Good; W=Wear out; P=Pitting; S= Scoring; F=Fracture. Table 6 shows the feature values obtained for the different worm specimens.
For defect identification, 150 sample images belonging to different categories were used for training the software. After training, the model was tested by using images from text samples.

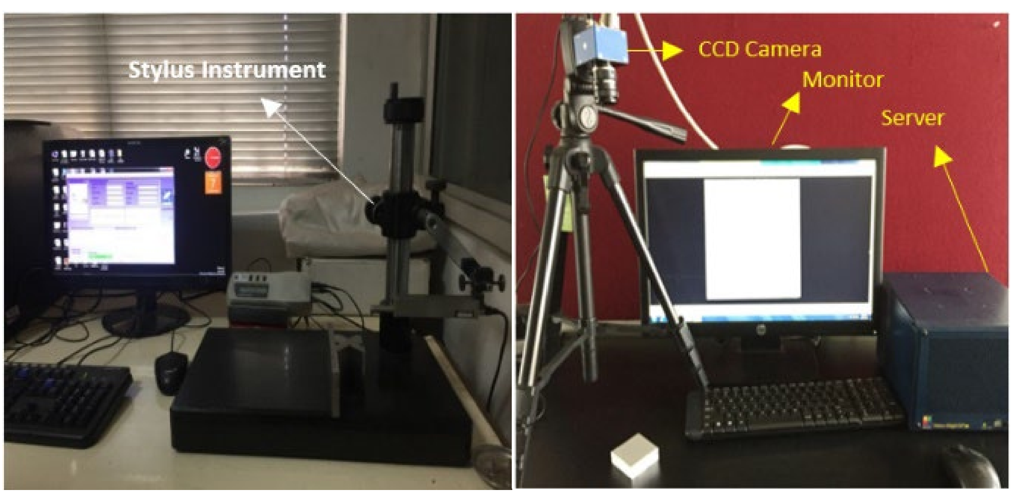

Fig. 2 Experimental Set-up of (a) stylus instrument (b) Vision system

4.Results analysis

Table 4 shows the measurements obtained from vision methods. The readings obtained from the vision system method are validated by comparing them with those obtained from conventional equipment.

Table 2 Digital image of a worm

189	187	178	171	168
167	171	180	188	156
165	178	177	185	182
183	167	166	176	175
190	174	175	180	182
165	166	176	154	176
156	145	143	165	162

Table 3 Digital image of the worm wheel

172	174	188	181	168
174	181	185	178	166
155	175	176	195	192
163	165	176	186	185
180	184	165	160	172
175	176	178	164	186
146	155	163	165	172

Table 4 Worm measurements comparison

Specimen	No. Threads		Pitch diameter (mm)		Tip diameter(mm)	
	Conventional method	Vision method	Conventional method	Vision method	Conventional method	Vision method
1	8	8	10.15	10.1523	11.95	11.9421
2	6	6	12.1	12.1432	13.6	13.5467
3	3	3	12.34	12.3434	14.34	14.3456
4	2	2	11.3	11.3564	12.8	12.8324
5	1	1	8.95	8.95234	9.95	9.95432

It is clear from Table 4 that the readings obtained from the vision approach are very close to the results obtained from the conventional gear measuring instruments. Table 5 shows the profile inspection result for different specimens used in the experimental investigation.

Table 5 Profile inspection result for different specimens (worm-wheel)

Specimen no	1	2	3	4	5	6	7	8
Result	A	R	RW	A	A	A	A	A

Note: A-Accept; R-Reject; RW-Rework

Table 6 Feature vectors of worm gears

Feature No.	1	2	3	4	5	6	7	8	9	10
FT1	2.93	2.67	2.97	2.86	2.86	2.97	2.97	2.97	2.82	2.97
FT2	0.11	0.08	0.08	0.34	0.38	0.14	0.15	0.15	0.07	0.16
FT3	0.84	0.59	0.77	1.05	1.09	0.94	0.96	0.98	0.96	1.06
FT4	2.01	2.14	2.78	1.87	2.38	2.36	2.74	2.64	2.58	2.58
FT5	0.56	0.55	0.57	0.46	0.46	0.56	0.46	0.53	0.57	0.59
FT6	1.06	1.04	1.63	0.94	0.94	0.97	1.08	1.06	1.04	0.97
FT7	1.37	1.46	1.36	0.98	0.93	1.38	1.63	1.47	1.34	1.37
FT8	55.4	53.8	51.7	58.6	57.2	54.3	51.4	51.4	51.6	53.6
FT9	1.35	1.45	0.86	1.37	1.37	0.94	1.35	0.98	0.98	1.34
FT10	5.55	5.24	4.27	5.78	5.78	5.82	4.87	4.24	5.69	5.78
FT11	0.06	0.06	0.07	0.27	0.18	0.05	0.24	0.27	0.27	0.49
FT12	0.67	0.57	0.56	0.64	0.68	0.64	0.55	0.59	0.57	0.69

Table 7 shows the confusion matrix obtained while conducting the classification experiment.

Table 7 Confusion Matrix

Training						Testing					
G	W	P	S	F	Classified as	G	W	P	S	F	Classified as
150	0	0	0	0	G	140	8	0	2	0	G
0	150	0	0	0	W	0	142	3	5	0	W
0	0	150	0	0	P	0	0	141	7	2	P
0	0	0	150	0	S	0	0	2	142	6	S
0	0	0	0	150	F	0	0	0	0	150	F

From Table 7, it is clear the software was trained using 150 sample images belonging to different categories. After training, the model's efficiency was tested using images from the test classes.

Out of 150 sample images of class 'Good,' 140 images were classified as belonging to the category 'Good.' In contrast, eight images were classified as belonging to the 'Wear' class, and two images belonged to the class Scoring. Thus, the classification accuracy was 93.33%.
Out of 150 sample images of class 'Wear out,' 142 images were classified as belonging to the category 'Wear out'', whereas three images were classified as belonging to the 'Pitting' class. And five images belonged to the class 'Scoring. Thus, the classification accuracy was 94.66%.

Out of 150 sample images of class 'Pitting, 141 images were classified as belonging to the class 'Pitting, whereas seven images were classified as belonging to the 'Scoring' category. Two images belonged to the class 'Fracture. Thus, the classification accuracy was 94%.

Out of 150 sample images of class 'Scoring, 142 images were classified as belonging to the class 'Scoring. Two images were classified as belonging to the 'Pitting' class and six shots belonging to the class 'Fracture. Thus, the classification accuracy was 94.66%.

Out of 150 sample images of class 'Fracture, 150 images were classified as belonging to the class Fracture,' and the classification accuracy was 100%.

5.Conclusion and directions for further research

The present research focuses on inspecting the worm and worm wheel using a vision system. The method presented here is non-contact type. The process is quick. The results obtained by the current approach were validated by comparing the results obtained from the conventional gear measuring instruments. The experimental investigation showed that the accuracy of the proposed method is 98%. The experiments were performed with the same specimen, and it was noticed that the repeatability of the current process is 99%. The research investigation revealed that the method could detect damaged teeth and other defects such as Wear, scoring, pitting, and fracture, with a classification accuracy of 93.33%, 94.66%, 94%, 94.66%, and 100%, respectively.

References

Goch, G. Gear Metrology, CIRP Annals, Volume 52, Issue 2, pp. 659-695, 2003. ISSN 0007-8506, https://doi.org/10.1016/S0007-8506(07)60209-1.

Vilmos V. Simon, Influence of tooth errors and shaft misalignments on loaded tooth contact in cylindrical worm gears, Mechanism and Machine Theory, Volume 41, Issue 6, Pp.707-724, 2006, ISSN 0094-114X, https://doi.org/10.1016/j.mechmachtheory.2005.09.004.

VDI/VDE 2608 Tangential composite and radial composite inspection of cylindrical gears, bevel, worm, and worm wheels. 2001.

AGMA 915-1-A02 Inspection Practices - Part 1: Cylindrical Gears - Tangential Measurements. 2002.

AGMA 915-2-A05 Inspection Practices - Part 2: Cylindrical Gears - Radial Measurements. 2005.

[a]Kiran, M.B., Additive manufacturing of titanium alloys-a review, Proceedings of the International Conference on Industrial Engineering and Operations Management, pp. 2553–2564 , 2021,

[b]Kiran, M.B., Lean transformation in electricity transmission tower manufacturing company-a case study, Proceedings of the International Conference on Industrial Engineering and Operations Management, pp. 2961–2974, 2021,

[c]Kiran, M.B., Productivity assessment studies in solenoid valve manufacturing company – a case study, Proceedings of the International Conference on Industrial Engineering and Operations Management, 2021, pp. 3037–3046.

[d]Kiran, M.B., A novel online surface roughness measuring method, Proceedings of the International Conference on Industrial Engineering and Operations Management, pp. 2907–2916, 2021,

Haralick, R.M., Shanmugam, K. and Dinstein, I. "Textural Features for Image Classification," in IEEE Transactions on Systems, Man, and Cybernetics, vol. SMC-3, no. 6, pp. 610-621, Nov. 1973, doi: 10.1109/TSMC.1973.4309314.

Thoen RL, Measuring base helix error on a sine bar, Gear Technology, pp. 25–27, 2001.

S. Hoover, Simplifying gear metrology, Quality, vol. 39, no.2, p. 48, 2000.

R. Moderow, Gear inspection, and measurement, Gear Technology, pp. 44-49, 1992.

E. Reiter, F. Eberle, Practical considerations for the use of double-flank testing for the manufacturing control of gearing-part I, Gear Technol, 31 (February), pp. 44-51, 2014.

K. Ni, Y. Peng, D. Stbener, G. Goch, Cylindrical Gear Metrology, W. Gao (Ed.), Metrology. Precision Manufacturing, pp. 1-29, 2019.

M.M. Auerswald, A. von Freyberg, A. Fischer, Laser line triangulation for fast 3d measurements on large gears Int J Adv Manuf Technol, 100 (9–12) (2019), pp. 2423-2433, 2019.

F. Balzer, M. Schäfer, I. Lindner, A. Günther, D. Stöbener, J. Westerkamp, Recent advances in optical gear measurements-a new approach for fast measurements of large gears, 6th International Conference on Gears, vol. 2255, VDI-Berichte, Garching (2015), pp. 655-666, 2015.

Biography

Dr. M.B. Kiran is an Associate Professor in the Department of Mechanical Engineering, School of Technology, Pandit Deendayal Petroleum University, Gandhinagar, Gujarat, INDIA. He earned his graduation (B.E.) from the University of Mysore in 1987. He did his post-graduation (M.E.) in Production Engineering from P.S.G. College of Technology (1991) and Doctoral degree (Ph.D.) in Surface Metrology from Indian Institute of Technology (I.I.T.), Madras in 1997. He has Industry/Research/Teaching experience of 25 years. He has published technical papers in many reputed national/international journals and conferences. He is a member of the Project management Institute (P.M.I.), U.S.A. He is a certified project manager (P.M.P.) from P.M.I. He has completed many mission-critical projects. He has conducted many training programs for working executives.